

Dynamic Modeling and Simulation of a Grid-Connected PV-wind hybrid Microgrid System Using MATLAB/SIMULINK

Ibrahim E. Abdulkafi¹, Abdelbaset M. Ihbal^{2*}.

1. Department of Electrical and Electronic Engineering. High institute for science and technology, Sabratha, Libya
2. Department of Electrical and Computer Engineering - School of Applied Science and Engineering The Libyan Academy for Postgraduate Studies, Tripoli, Libya

ABSTRACT

Hybrid renewable Energy System (HRE) in a system configured with renewable energy sources requires storage facilities or backup generation to maintain continuity of supply to loads when the renewable energy sources alone are not sufficient. HRE systems are widely familiar as efficient power generation mechanisms due to their low operating costs, high reliability, and flexibility in grid-connected operations. This paper presents and investigate a model a Grid-Connected PV-wind hybrid Microgrid (MG) System. The system consists of a PV system, a wind turbine and an ultracapacitor as an energy storage element. All generation units have been connected to the distribution network to run in grid-connected mode. Maximum Power Point Tracking (MPPT) has been adopted to increase the power output then array efficiency of PV systems. For short-term transient simulations, dynamic models are developed for each system module. Utilizing MATLAB/Simulink, the simulated test-bed is created. Simulations are used to examine the test-bed's behaviors during steady state, abrupt variations in wind speed, and when facing a line fault. The outcomes of this study demonstrated that DER, UCESS, as well as the proposed control technique all support system stability under transient disturbance. The developed model might be seen as an effective tool for enhancing the functionality of the grid.

KEYWORDS: *renewable energy source; grid-connected; hybrid AC/DC microgrid; MPPT; distribution network;*

I. INTRODUCTION

Increased power demand will drive the deployment of energy storage (ES) and power generation at distribution level. Distributed Energy Resources (DERs) are small-scale energy sources that can be harvested to deliver reliable and efficient electricity to meet a regular demand of consumers, usually in close proximity to consumers. will be split. [1]. Most distributed energy sources are connected to the power grid and consumer loads via DC-AC voltage inverters. DER systems typically use renewable energy sources such as solar, small hydro, biogas, wind, and biomass [2, 3]. However, due to the intermittent nature of renewable energy, it requires the support of an Energy Storage System (ESS) to provide ancillary services and store excess energy for later use. ESS policies have been proposed in some countries to support renewable energy integration and grid stability. A microgrid (MG) can be easily achieved by simply installing distributed power resources to supply power to on-site consumers. DER, energy storage system and load define a microgrid that can operate in parallel with

the main grid (grid-tied mode) or independently. Microgrids (MG) have been applied in several practical

areas such as industrial use, remote areas, residences, and commercial buildings [3, 4, 5, 6, 7]. The two most well-known sources of electrical distributed energy resources are wind turbines and solar power. Batteries, superconducting coils, flywheels, or supercapacitors are common energy storage devices used in numerous applications because of their rapid load acceptance and capability of storing and releasing energy within a short duration of time [8]. Microgrids can be confidential as DC microgrids, AC microgrids, or hybrid AC/DC grids [9]. Wind turbines are alternating current (AC) power sources, while ultracapacitors solar cells and are direct current (DC) devices. Figure 1 shows the main components of a solar and wind hybrid energy system. The DC and AC microgrids are both combined to form a hybrid microgrid. control strategies and bidirectional power electronics are needed to govern hybrid AC/DC grids to attain stable performance while connected to the AC utility grids [10]. Dynamic modeling of MG is performed to study steady-state and transient responses. Modeling includes storage systems, energy resources, controllers and power electronics devices. The purpose of this study is to create a complete model of the microgrid including power sources, its power

* Corresponding author: A.Ihbal@academy.edu.ly

electronics, controls and steady-state loads to study transient behavior with changing inputs. The system is simulated in his MATLAB/Simulink. The evaluation of results is discussed.

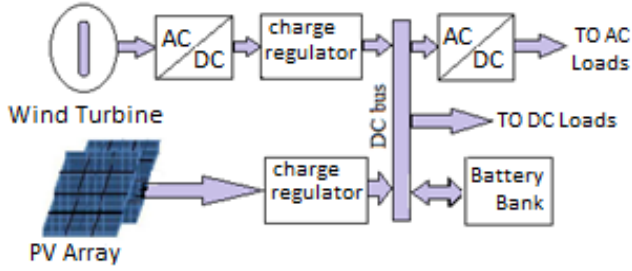


Fig 1: Hybrid Energy System Components

II. GRID-TIED PV - WIND HYBRID GENERATION MICROGRID MODELING

This section describes the formation of a grid-tied hybrid AC/DC microgrid for a hybrid solar and wind turbine power generation system. The proposed system consisting of a wind turbine, a photovoltaic array, a DC/DC converter with an isolation transformer that ensures that the photovoltaic array operates at its MPP, a DFIG, and an ultracapacitor ESS and AC /DC/AC thyristor-controlled double-bridge converters is shown in Figure 2. The system frequency is 50Hz and the rated voltage is 400V.

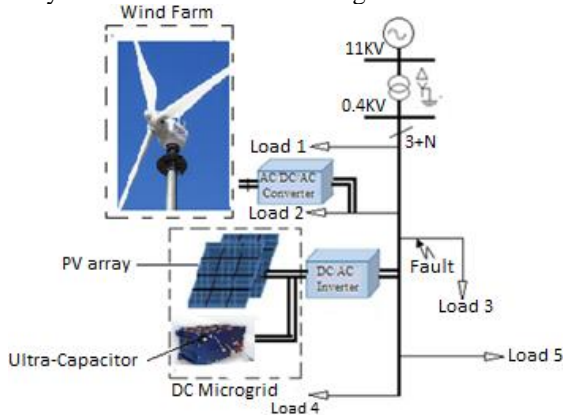


Fig.2. Grid-connected PV- wind hybrid AC/DC microgrid

III. MODELING OF DC MICROGRID

Figure 3 shows the structure of the DC microgrid. Here, a PV array and an energy storage device are connected to a DC bus, which is connected to the grid through an inverter.

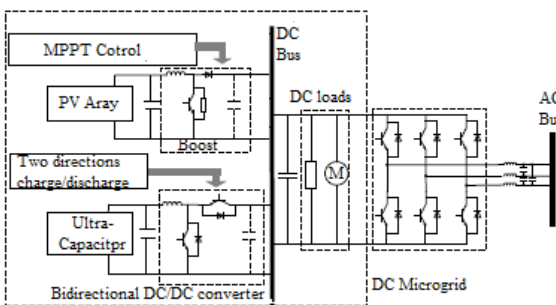


Fig. 3. Structure of the DC microgrid.

The PV arrays have boost converters and linked to a common DC bus. The ultracapacitors are similarly connected to a common DC bus via bidirectional DC/DC converters. DC motors and DC resistors are the two different types of DC load. PV power units are managed to produce a maximum power.

A. MATHEMATICAL MODEL FOR PHOTOVOLTAIC CELL

Solar cells are basically pn junctions fabricated on thin semiconductor wafers. Electromagnetic radiation from solar energy can be converted directly into electricity by the PV effect. When a semiconductor is exposed to sunlight, photons with energies larger than the semiconductor's bandgap energy cause a proportional number of electron-hole pairs to form. Figure. 4 below shows the equivalent circuit of a solar cell.

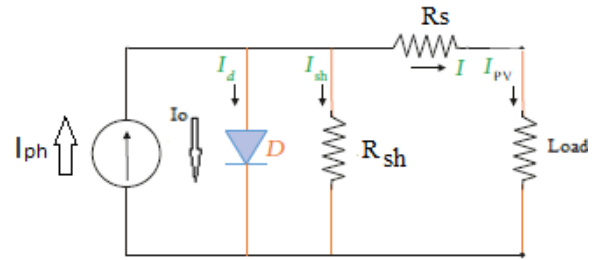


Fig 4. Single-diode solar cell equivalent circuit

The current source I_{ph} represents the cell photocurrent. R_s and R_{sh} are the inherent series and shunt cell resistances respectively. Usually, the value of R_{sh} is very large and the value of R_s is very small and can be ignored for simplicity of analysis. [11]. PV cells are grouped into large units called PV modules and connected in a parallel-series configuration to form a PV array. A photovoltaic module can be mathematically modeled as in equations (1)-(4). [12-14].

Photo-current of the module I_{ph} :

$$I_{ph} = [I_{scr} + K_i(T - 298)] * \lambda / 1000 \quad (1)$$

Reverse saturation current of the module I_{rs} :

$$I_{rs} = I_{scr} / [\exp(qV_{OC} / N_s K A T) - 1] \quad (2)$$

The module saturation current I_0 changes with the temperature of the cell, that is given by

$$I_0 = I_{rs} \left[\frac{T}{T_r} \right]^3 \exp \left[\frac{q^* E_{g0}}{B K} \left\{ \frac{1}{T_r} - \frac{1}{T} \right\} \right] \quad (3)$$

The current output of PV module is

$$I_{PV} = N_p * I_{ph} - N_p * I_0 \left[\exp \left\{ \frac{q^*(V_{PV} + I_{PV} R_s)}{N_s A K T} \right\} - 1 \right] \quad (4)$$

Where:

k : Boltzmann constant = 1.3805×10^{-23} J/K

λ : tip speed ratio

T : Module operating temperature in Kelvin,

I_{scr} : PV module short-circuit current at 25°C,

λ : PV module illumination (W/m^2) = $1000 W/m^2$,

q : Electron charge = 1.6×10^{-19} C,

A : An ideality factor

E_{g0} : silicon band gap = 1.1 eV,

B : An ideality factor,

T_r : Reference temperature = 298 K,

The current output of PV module I_{PV} is

N_s : number of series-connected cells., N_p - number of parallel connected cells.

V_{pv} : PV module output voltage (V),

R_s : PV module series resistance of,

$$V_{oc} = V_{pv}, 36 = N_s = \& N_p = 1$$

The specifications of the proposed PV models (including PV manufacturing datasheets) are exposed in

Table I. Electrical SpecificationS for Solar PanelS at 1.5AM, 25 °C, 1000W/m2

Parameters		Value
Max power rating (Pmax)	[W]	55
Impp (Rated)	[A]	3.15
Vmpp (Rated)	[V]	17.4
Isc	[A]	3.45
Voc	[V]	21.7
No. of Cells /module		36
No. of modules connected in series / string		24
No. of parallel strings		12

B. MAXIMUM POWER POINT TRACKING (MPPT)

MPPT is a method commonly used in PV solar systems to maximize power production regardless of the environment [10]. Figure 5 shows the MPPT tracking circuit.

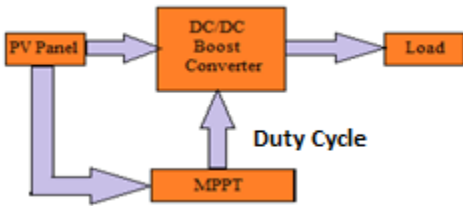


Fig.5. Circuit Arrangement of MPPT

By altering the IGBT's duty cycle in the converter for boost, MPPT can be matched. MPPT aims to use control algorithms to confirm that the PV system is working at the MPPT. The Perturbation & Observation (P&O) technique is one of the most commonly used MPPT methods, due to its simplicity and less requirements for measured variables. The P&O algorithm constantly measures the current and voltage at the solar array terminals, constantly perturbs the voltage with small perturbations, and observes the change in output power to determine the next control signal. If the output power rises, the disturbance continues in similar way in the next step, otherwise the direction of the disturbance is reversed. To improve the tracking speed and accuracy of the algorithm, the perturbations should be continuously adjusted [10].

Observing the PV cell characteristics curve satisfy the following slope of the PV curve equations: equation

$$\left(\frac{dP}{dV} = 0\right)$$

determines whether the PV module's operating point is at the MPP. On the other hand, equations

$\left(\frac{dP}{dV} < 0\right)$ act on the left and right sides of the well-defined operating point of the PV curve.

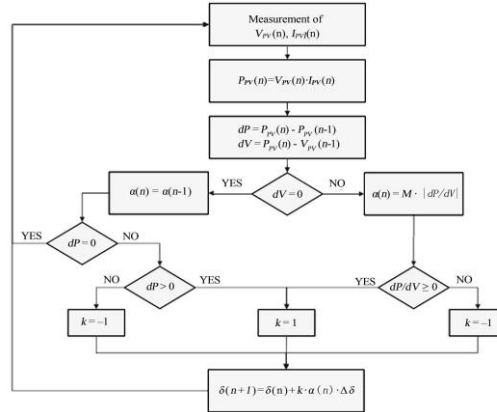


Fig 6. Flow-chart for variable-step P&O method.

C. UC ENERGY STORAGE SYSTEMS

Ultracapacitors (UC) are energy storage devices that have lifetimes exceeding 1,000,000 charge-discharge cycles, high power densities, great reliability, almost instantaneous charging and discharging, tolerance to extreme temperatures, and high efficiency.

1) UC MODEL

UC model consists of a series resistor (ESR), an ideal capacitor, and a shunt resistor (EPR). The ESR is small, simulating heat loss and transient charge/discharge voltage mutations in the discharge/charge process. EPR with a large resistor represents current leakage impact and affects long term energy storages. The classical model for UC is represented in Figure 7.

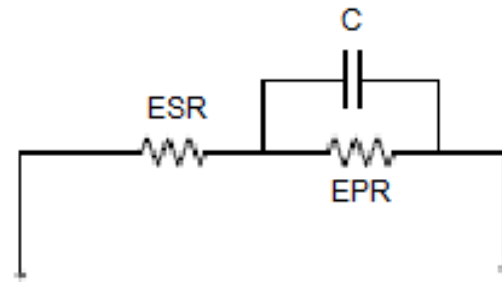


Fig 7 Classical model for UC.

2) BIDIRECTIONAL DC-DC CONVERTER CONTROL SYSTEM

UC energy storage consists of an UC, a bidirectional DC to DC converter and a control system. This configuration should allow the ultracapacitor to operate in bidirectional mode. The bidirectional converter control system is shown in Figure 8. The main goal is to keep the voltage of the common dc link circuit constant [15]. In this manner, the voltage of the common dc link remains stable regardless of whether the ultracapacitor is being charged or discharged, resulting in the lowest capacitor voltage ripple.

When the DC-link voltage is less than the reference, switch S2 becomes active and the converter operates similar to that of boost converters. When the DC-link voltage is greater

than the reference, switch S1 becomes active and the converter operates similar to that of buck circuit. In case of steady state, the input and output voltages satisfy the following relationships:

$$V_{dc} = \frac{V_{uc}}{1-D_1} = \frac{V_{uc}}{D} \quad (\text{Boost}) \quad (5)$$

$$V_{uc} = D_2 V_{dc} = D V_{dc} \quad (\text{Buck}) \quad (6)$$

Where, D is the switching signal duty cycle.

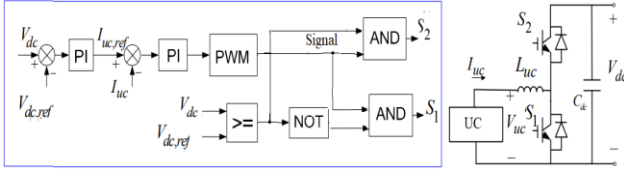


Fig 8. Control of Bidirectional DC- DC converter [10].

IV. MODELING OF AC MICROGRID

A. MODELING OF WIND POWER GENERATION SYSTEM

Most wind power systems use variable speed pitch-controlled wind turbines with doubly fed induction generators (DFIGs). This is because it has some advantages over other types of wind turbine generators such as conversion of wind energy with high efficiency and control of both reactive and active power, decrease power fluctuations and produce high-quality of power [16,17]. The basic structure of a grid-connected DFIG wind turbine is shown in Figure 9. The rotor is powered by an AC/DC/AC converter and the stator is directly connected to the 50 Hz grid.

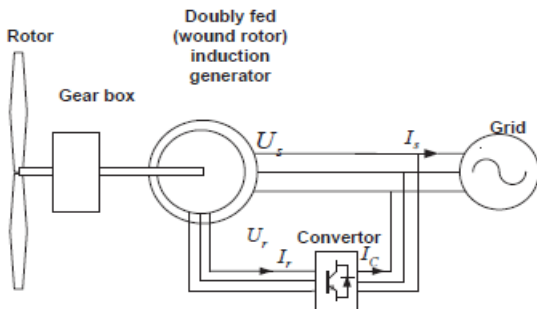


Fig 9 . Arrangement of the DFIG wind power [18].

Table 2: Wind POWER generation Specification

Parameters	Value
Rated power (KW)	60
Diameter (m)	5.6
No. of blades	3
Rated wind speed (m/s)	15
Generator Rating (KW)	15
No. of turbines	4

1. MODEL OF WIND TURBINE

The wind turbine's generated mechanical power can be expressed as:

$$P_m = 0.5 \rho A \cdot C_p(\lambda, \beta) \cdot v_w^3 \quad (7)$$

where ρ is the air density in Kg/m³, $A = \pi R^2$ is the swept area of wind turbine in m², v_w is wind speed in (m/s), C_p is the power coefficient that is a function of a tip speed ratio (λ) and the pitch angle of blade β . The $C_p(\lambda, \beta)$ is the measurement of the amount of wind energy that a turbine could capture. To model $C_p(\lambda, \beta)$ [18-20]., the following expression is employed.

$$C_p(\lambda, \beta) = 0.5176 \cdot \left(\left(\frac{116}{\lambda + 0.08\beta} - \frac{4.06}{\beta^2 + 1} \right) - 0.4\beta - 5 \right) \cdot e^{-\lambda^2} + 0.0068\lambda \quad (8)$$

The electromechanical equations of motion of shaft system are:

$$T_{wt} = J_{wt} \frac{d\omega_{wt}}{dt} + D_{wt}(\omega_{wt} - \omega_{gen}) + H_{wt}(\theta_{wt} - \theta_{gen})$$

$$\frac{d\theta_{wt}}{dt} = \omega_{wt} \quad (9)$$

$$-T_{gen} = J_{gen} \frac{d\omega_{gen}}{dt} + D_{gen}(\omega_{gen} - \omega_{wt}) + H_{gen}(\theta_{gen} - \theta_{wt}) \frac{d\theta_{gen}}{dt} = \omega_{gen} \quad (10)$$

Where, H_{wt} and H_{gen} are stiffness coefficients of the turbine and the generator. ω_{wt} and ω_{gen} are the rotational speeds of the generator and the turbine, respectively, in rad/s; T_{wt} and T_{gen} are the torques of the turbine and the generator; J_{gen} and J_{wt} are the moments of inertia of the generator and the turbine, respectively; D_{gen} and D_{wt} are the coefficients of linear damping of the both generator and turbine; and H_{gen} and H_{wt} are the coefficients of stiffness for the generator and the turbine.

2. MODELING OF INDUCTION GENERATOR

Figure 10 illustrates the induction machine's electrical circuit in reference frame (dq frame).

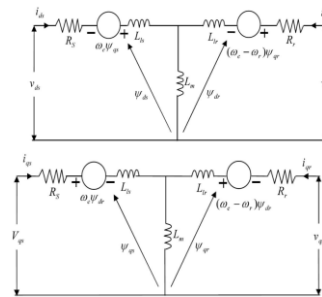


Fig 10. Electrical circuit for the induction machine in reference frame

The following set of equations can be used to compute the voltage and flux linkage.:

$$v_{sd} = R_{sd} i_{sd} - \omega_s \psi_{sd} + \frac{d\psi_{sd}}{dt} \quad (11)$$

$$v_{sq} = R_{sq} i_{sq} + \omega_s \psi_{sq} + \frac{d\psi_{sq}}{dt} \quad (12)$$

$$v_{rd} = R_{rd} i_{rd} - (\omega - \omega_r) \psi_{rd} + \frac{d\psi_{rd}}{dt} \quad (13)$$

$$v_{rq} = R_{rq} i_{rq} + (\omega - \omega_r) \psi_{rq} + \frac{d\psi_{rq}}{dt} \quad (14)$$

The flux (ψ) equation are

$$\psi_{sd} = l_s i_{sd} + l_m i_{rd} \quad (15)$$

$$\psi_{sq} = l_s i_{sq} + l_m i_{rq} \quad (16)$$

$$\psi_{rd} = l_r i_{rd} + l_m i_{sd} \quad (17)$$

$$\psi_{rq} = l_r i_{rq} + l_m i_{sq} \quad (18)$$

Where v_{sd} and v_{sq} are d-axis and q-axis stator voltages, i_{sd} and i_{sq} are the d-axis and q-axis stator currents, and ω is the arbitrary reference frame's electromechanical, ω_s is the synchronous speed, while ω_r is the speed of the rotor. R_{sd} is the stator resistance d-axis, R_{sq} is the stator resistance q-axis, R_{rd} is the rotor resistance d-axis, R_{rq} is the rotor resistance q-axis. ψ is permanent flux, l_s , l_r and l_m are the stator self-inductance, rotor self-inductance and mutual inductances of the generator respectively.

3) CONTROL SYSTEM OF WIND GENERATION

Generation system of wind turbine control comprises of wind turbine control, rotor-side converter control, and grid-side converter control [21-24]. The purpose of controlling a wind turbine is to obtain mechanical energy from the wind. Active and reactive power are managed at the stator terminal via rotor-side converter control. Regardless of the size and direction of rotor power, grid-side converter control keeps the dc link voltage constant.

There is a specific rotational speed that can be reached at the intended wind speed in order to maximize the power coefficient and, thus, extract the most mechanical power possible from the available wind power. A wind turbine's output power and speed are regulated using a pitch angle control system [18]. The rotational speed is altered when the wind speed is less than the rated value such that the power coefficient maintains maximum when the pitch angle is zero. In contrast, PI controllers are utilized for pitch angle to limit the mechanical power if wind speed climbs over the rated value. An example of a typical pitch angle control system is shown in Figure 11.

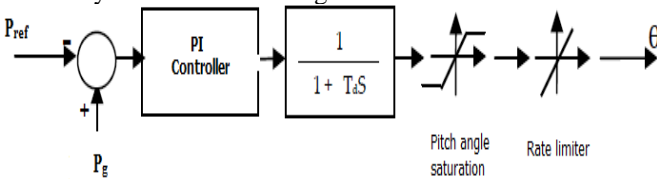


Fig 11. Control system of conventional pitch angle

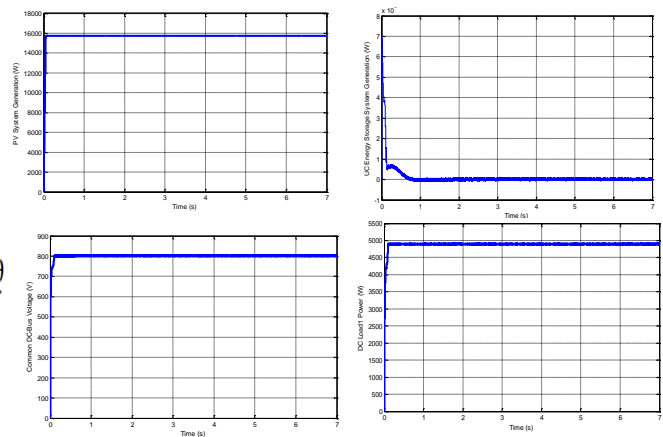
V. RESULTS AND DISCUSSIONS OF GRID-TIED HYBRID AC/DC MICROGRID SIMULATION

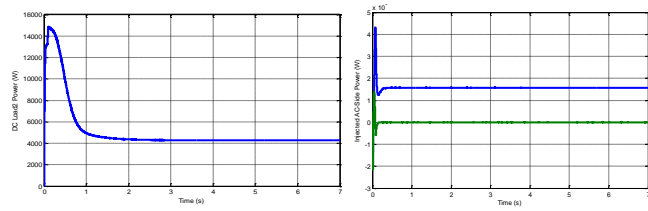
In a hybrid energy system, two or more renewable and nonrenewable energy sources are often combined. (Wind power and solar energy are consistently combined into a hybrid system, especially for the power supply for remote places where the expense of a transmission line is too expensive. The primary justification for choosing solar and wind energy is that they both fluctuate throughout the day; however, when they are combined, one can make up for the other, increasing system dependability.

Simulink in MATLAB is used to model the compact hybrids grid in detail and simulate system operations. It is seen in Figure 2. Three diverse scenarios, including steady-state operation, fluctuating solar irradiation, and a 3ph short circuit line fault, were investigated using the created model.

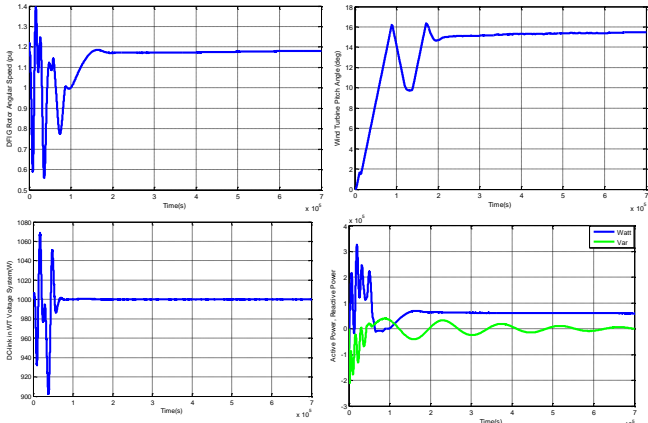
A. STEADY STATE OPERATION

In steady state scenario, the entire distributed generation units operate at nominal values, providing power to both the grid and the load. A preliminary stability analysis was carried out to highlight the paper's goal. The PV system is supplying enough electric power to the consumers (load) and grid, While the ultracapacitor energy storage system (UCESS) is inactive (not in use), meaning they are not being charged or discharged. The output of the PV and wind systems differs. The PV system produces DC output, which needs to be converted to AC prior to being connected to the grid. We employ a variety of power electronic interface devices for purpose. The simulation results for the steady state operation are shown in Figure 12. From this figure it can be seen that the distributed generation units quickly reached steady state operation (after just a short amount of time). Figure 12 (b) for the active power for the loads shows that the three distributed generation units are able to power the nearby loads, but that the voltage sag brought on by line reactance losses prevents the distant loads from receiving their nominal power.





(a) DC Microgrid: PV system power generation, UCESS power generation, DC common bus voltage, DC load 1 power, DC load 2 power, AC power supplied to power grid.



(b) Wind power system: PCC reactive and active power, dc-link voltage, and DFIG angular speed and wind turbine pitch angle
 Fig. 12 Simulation results for the system at steady-state.

B. TRANSIENTS OF SOLAR IRRADIANCE

Another test was run with a step adjustment in the sun irradiation from 1000 W/m² to 1300 W/m². At t=2s and t=4s, it changes back from 1300 W/m² to 800 W/m², respectively. Cell temperature remains constant at 298 K during this time. The PV system's simulation results were shown in Figure 13. During the time period t=2s–4s, solar irradiation causes an increase in PV power generation, which is used to charge the UC energy storage system. During the time period t=4s–7s, PV output generation drops with solar irradiation and UC is discharged to power demands. Due to the system's usage of UC energy storage, DC and AC loads are not impacted by PV power fluctuations during this time.

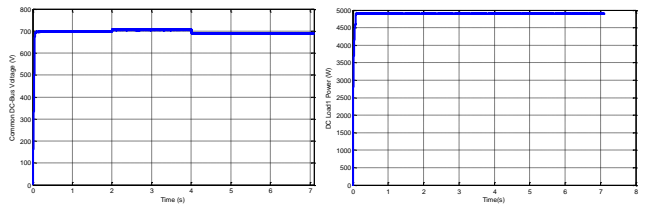
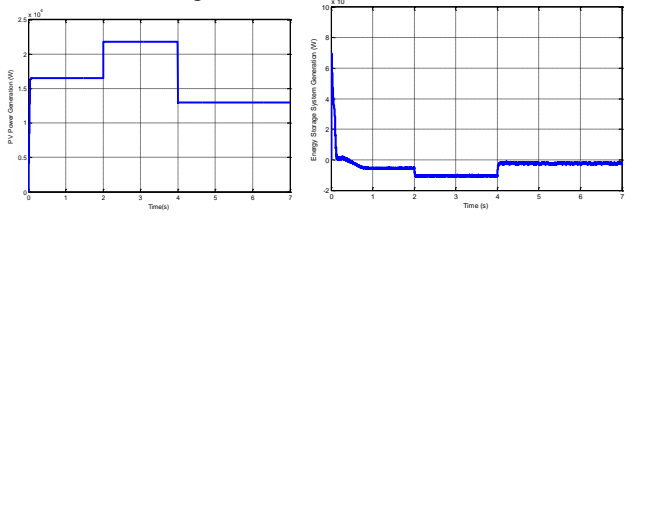
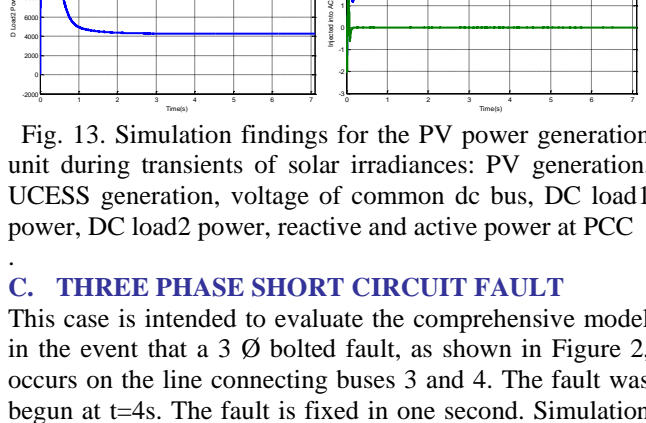


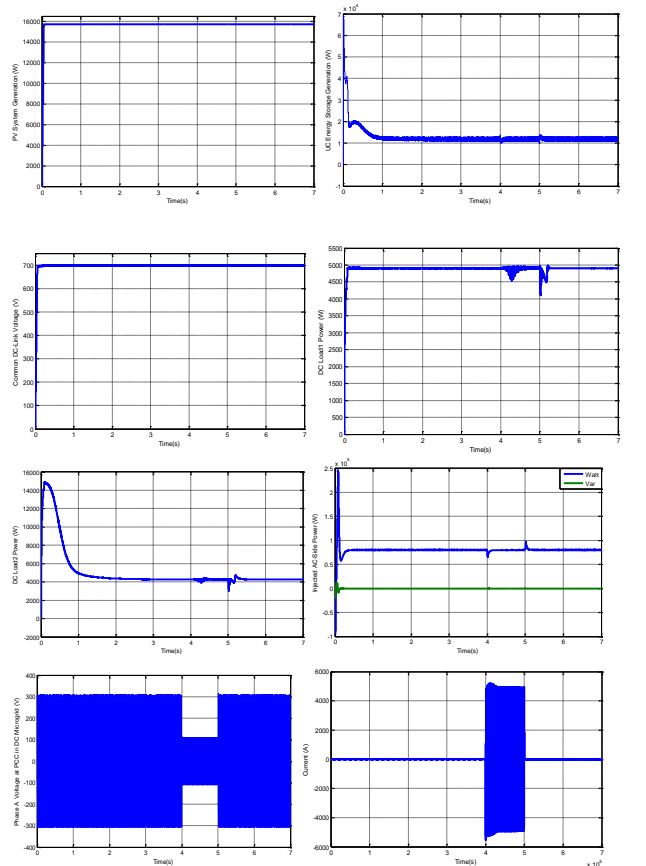
Fig. 13. Simulation findings for the PV power generation unit during transients of solar irradiances: PV generation, UCESS generation, voltage of common dc bus, DC load 1 power, DC load2 power, reactive and active power at PCC



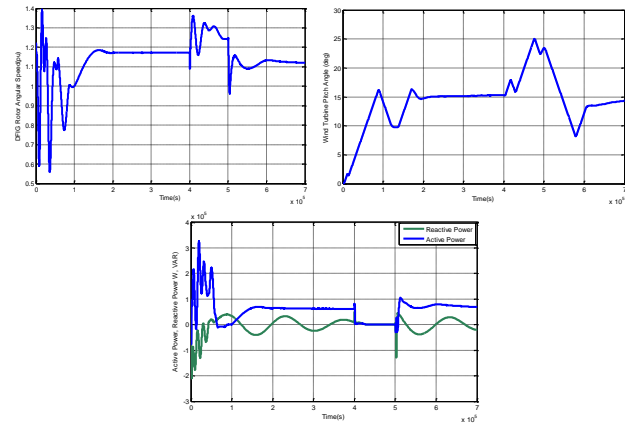
(b) Wind power system: PCC reactive and active power, dc-link voltage, and DFIG angular speed and wind turbine pitch angle
 Fig. 12 Simulation results for the system at steady-state.

C. THREE PHASE SHORT CIRCUIT FAULT

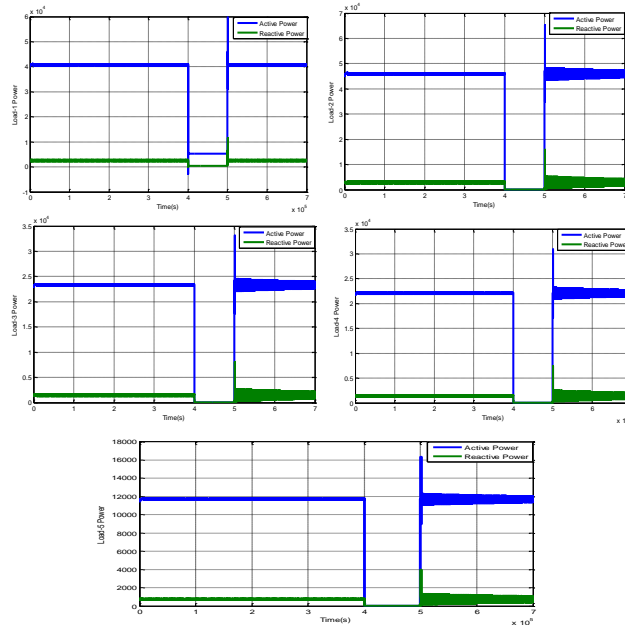
This case is intended to evaluate the comprehensive model in the event that a 3 Ø bolted fault, as shown in Figure 2, occurs on the line connecting buses 3 and 4. The fault was begun at t=4s. The fault is fixed in one second. Simulation results are shown in Figure 14. The entire system is unstable throughout the fault phase (4s–5s). Actually, due to the fault, the DC microgrid is cut off from the grid. All distributed generation units return to normal and run steadily after the issue is fixed after a period of five seconds. When the fault is fixed, the system can continue to be stable as a whole.



(a) DC microgrid (MG) system: PV power generation, UCESS, DC common bus voltage, DC loads 1 and 2, AC power supplied to grid, phase A current and voltage of PCC



(b) Wind power system: pitch angle of turbine DFIG angular velocity, PCC reactive and active power.



(c) Reactive and active power of five loads in the power network.

Fig 14. Simulation findings at fault occurrence

VI. CONCLUSIONS

In this paper, a grid-connected PV-wind hybrid microgrid system has been described. For short-term transient simulations, a detailed dynamic modeling of the system is investigated, including device and network-level control techniques. Based on the findings of this study, it is possible to draw the following conclusions can be drawn: Each distributed generation unit runs steadily and feeds electricity to the consumers (loads). These devices support voltage maintenance (minimize voltage sag) and supply sufficient power to nearby loads Similar DFIG transients are caused by fluctuations in wind speed, but the control system of pitch angle modifies the pitch angle to capture the greatest wind power when the

wind speed is below the nominal value and cap the output power to safeguard the device when the wind speed is above the nominal value.

The PV generation changes as a result of variations in solar irradiation; however, the PV system tracks the maximum power point under each circumstance.

Ultracapacitors enhance overall system stability. currents and Voltages are influenced by the 3-phase fault. The rotational speed of the wind turbine system fluctuates during this time.

The operation of the DC microgrid is not significantly impacted by the fault since the bidirectional converter in the UCESS system is managed to keep DC bus voltages nearly constant during faults. Overall, simulation results have shown that the suggested control approach, DER, and UCESS all contribute to system stability during transient disturbances.

The created model could be considered as a useful tool for improving the performance of smart grids.

Further studies on combining other hybrid systems with this existing system such as batteries or fuel cell system can be investigated

REFERENCES

- [1] Laaksonen, H.J. 2010. Protection Principles for Future Microgrids. IEEE Transactions on Power Electronics, 25(12): 2910–2918.
- [2] S. Chowdhury, S. Chowdhury, and P. Crossley, Microgrids and active distribution networks. Institution of Engineering and Technology, 2009.
- [3] Justo, J.J., Mwasilu, F., Lee, J. & Jung, J.-W. 2013. AC-microgrids versus DC-microgrids with distributed energy resources: A review. Renewable and Sustainable Energy Reviews, 24: 387–405.
- [4] C. Yuan, M. A. Haj-Ahmed, and M. S. Illindala, “Protection strategies for medium-voltage direct-current microgrid at a remote area mine site,” IEEE Transactions on Industry Applications, vol. 51, no. 4, pp. 2846–2853, 2015.
- [5] J. Tian, Z. Liu, J. Shu, J. Liu, and J. Tang, “Base on the ultra-short term power prediction and feed-forward control of energy management for microgrid system applied in industrial park,” IET Generation, Transmission & Distribution, vol. 10, no. 9, pp. 2259–2266, 2016.
- [6] M. Hong, X. Yu, N.-P. Yu, and K. A. Loparo, “An energy scheduling algorithm supporting power quality management in commercial building microgrids,” IEEE Transactions on Smart Grid, vol. 7, no. 2, pp. 1044–1056, 2016.
- [7] D. Zhang and J. Wang, “Research on construction and development trend of micro-grid in china,” Power System Technol, vol. 40, no. 2, pp. 451–458, 2016.
- [8] P. Ribeiro, B. Johnson, M. Crow, A. Arsoy, and Y. Liu, “Energy storage systems for advanced power applications,” Proceedings of the IEEE, vol. 89, no. 12, pp. 1744–1756, 2001.
- [9] Justo, J.J., Mwasilu, F., Lee, J. & Jung, J.-W. 2013. AC-microgrids versus DC-microgrids with distributed energy

- resources: A review. *Renewable and Sustainable Energy Reviews*, 24: 387–405.
- [10] Fei Ding; Loparo, K.A. ; Chengshan Wang “Modeling and simulation of grid-connected hybrid AC/DC microgrid” *Power and Energy Society General Meeting, 2012 IEEE 2012*, Page(s): 1 – 8.
- [11] N. Pandiarajan, and Ranganath Muthu, “Mathematical Modeling of Photovoltaic Module with Simulink,” *International Conference on Electrical Energy Systems (ICEES 2011)*, Jan 2011.
- [12] S. Chowdhury, S. P. Chowdhury, G.A. Taylor, and Y.H.Song, “Mathematical Modeling and Performance Evaluation of a Stand-Alone Polycrystalline PV Plant with MPPT Facility,” *IEEE Power and Energy Society General Meeting - Conversion and Delivery of Electrical Energy in the 21st Century*, July 20-24, 2008, Pittsburg, USA.
- [13] Jee-Hoon Jung, and S. Ahmed, “Model Construction of Single Crystalline Photovoltaic Panels for Real-time Simulation,” *IEEE Energy Conversion Congress & Expo*, September 12-16, 2010, Atlanta, USA.
- [14] S. Nema, R. K. Nema, and G.Agnihotri, “Matlab simulink based study of photovoltaic cells / modules / array and their experimental verification,” *International Journal of Energy and Environment*, pp.487- 500, Volume 1, Issue 3, 2010.
- [15] A. M. O. Haruni, A. Gargoom, M. E. Haque, M. Negnevitsky, “Dynamic Operation and Control of a Hybrid Wind-Diesel Stand Alone Power Systems,” *Applied Power Electronics Conference and Exposition*, 2010.
- [16] E.Spahic, J. Morren, G. Balzer, and G. Michalke, “Mathematical model of the double fed induction generator for wind turbines and its control quality,” *POWERENG 2007*, April, Portugal.
- [17] F. D. Kanellos, N. D. Hatziaargyriou, “Optimal Control of Variable Speed Wind Turbines in Islanded Mode of Operation,” *IEEE Trans. Energy Conversion*, vol. 25, no.4, pp. 1142-1151, Dec. 2010.
- [18] Faisal Mohamed. *Microgrid Modelling and Simulation*. PhD thesis, 2006.
- [19] Indrajit Koley, Swarnankur Ghosh, Avishek Ghose Roy, Pradip Kumar Saha and Gautam Kr. Panda Matlab “Modeling and Simulation of Grid Connected Wind Power Generation Using Doubly Fed Induction Generator” *International Journal of Computational Engineering Research*, ISSN (e): 2250 – 3005 Vol, 04 Issue, July – 2014.
- [20] Siegfried Heier, “Grid Integration of Wind Energy Conversion Systems,” *John Wiley & Sons Ltd*, 1998.
- [21] Wei Qiao, “Dynamic modeling and control of double fed induction generators driven by wind turbines,” *Power System Conference and Exposition, 2009, PSCE’09. IEEE/PES*.
- [22] N. Gyawali, Y. Ohsawa, O. Yamamoto, “Dispatchable power from DFIG based wind-power system with integrated energy storage”, *Power and Energy Society General Meeting, 2010 IEEE*.
- [23] Seul-Ki Kim, Jin-Hong Jeon, Chang-Hee Cho, et al, “Modeling and simulation of a grid-connected PV generation system for electromagnetic transient analysis,” *Solar Energy*, vol. 83, no.4, 2009.
- [24] M. C. Cavalcanti, G. M. Azevedo, B. A. Amaral, et al. “Efficient Evaluation in Grid Connected Photovoltaic Energy Conversion Systems,” *IEEE Annual Power Electronics Specialists Conference*, 2005.